










# Cardiac computed tomography following Watchman FLX implantation: device-related thrombus or device healing?

Anders Dahl Kramer <sup>1</sup>, Kasper Korsholm <sup>1</sup>, Jesper Møller Jensen <sup>1</sup>,  
Bjarne Linde Nørgaard <sup>1</sup>, Srikara Peelukhana<sup>2</sup>, Thomas Herbst<sup>2</sup>,  
Rodney Horton <sup>2,3</sup>, Saibal Kar <sup>2,4</sup>, Jacqueline Saw <sup>5</sup>, Mohamad Alkhouli <sup>6</sup>,  
and Jens Erik Nielsen-Kudsk <sup>1\*</sup>

<sup>1</sup>Department of Cardiology, Aarhus University Hospital, Palle Juul-Jensens Boulevard 99, 8200 Aarhus N, Denmark; <sup>2</sup>Research and Development, Boston Scientific, Maple Grove, MN, USA; <sup>3</sup>Texas Cardiac Arrhythmia Institute, Austin, TX, USA; <sup>4</sup>Los Robles Regional Medical Center, Thousand Oaks, CA, USA; <sup>5</sup>Division of Cardiology, Vancouver General Hospital, British Columbia, Canada; and <sup>6</sup>Department of Cardiovascular Diseases, Mayo Clinic School of Medicine, Rochester, MN, USA

Received 9 August 2022; accepted 7 October 2022; online publish-ahead-of-print 7 November 2022

## Aims

Cardiac computed tomography (CT) is increasingly utilized during follow-up after left atrial appendage closure (LAAC). Hypoattenuated thickening (HAT) is a common finding and might represent either benign device healing or device-related thrombosis (DRT). The appearance and characteristics of HAT associated with the Watchman FLX have not been previously described. Therefore, we sought to investigate cardiac CT findings during follow-up after Watchman FLX implantation with a focus on HAT and DRT.

## Methods and results

Retrospective single-centre, observational study including all patients with successful Watchman FLX implantation and follow-up cardiac CT between March 2019 and September 2021 ( $n = 244$ ). Blinded analysis of CT images was performed describing the localization, extent, and morphology of HAT and correlated to imaging and histology findings in a canine model. Relevant clinical and preclinical ethical approvals were obtained.

Overall, HAT was present in 156 cases (64%) and could be classified as either subfabric hypoattenuation ( $n = 59$ ), flat sessile HAT ( $n = 78$ ), protruding sessile HAT ( $n = 16$ ), or pedunculated HAT ( $n = 3$ ). All cases of pedunculated HAT and five cases of protruding sessile HAT were considered as high-grade HAT ( $n = 7$ ). Subfabric hypoattenuation and flat sessile HAT correlated with device healing and endothelialization in histological analysis of explanted devices.

## Conclusion

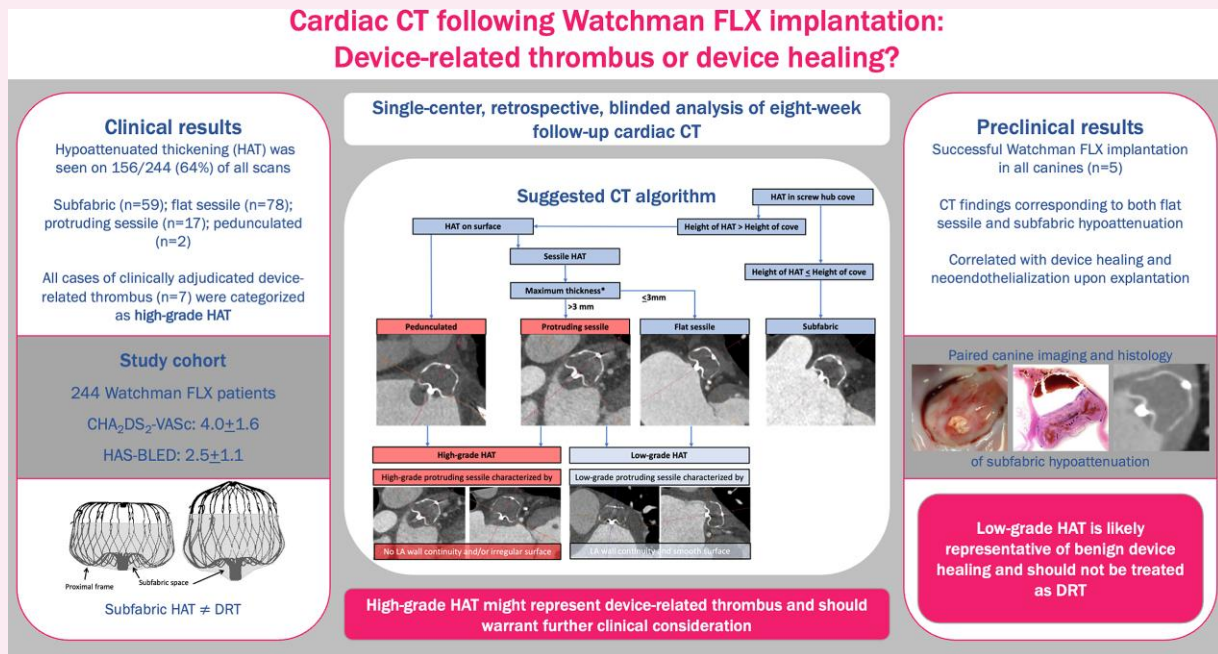
Subfabric hypoattenuation and flat sessile HAT are frequent CT findings for Watchman FLX, likely representing benign device healing and endothelialization. Pedunculated HAT and protruding HAT are infrequent CT findings that might represent DRT.

\* Corresponding author. Phone: +45 30922341, Fax: +45 78452260, E-mail: je.nielsen.kudsk@gmail.com

© The Author(s) 2022. Published by Oxford University Press on behalf of the European Society of Cardiology.

This is an Open Access article distributed under the terms of the Creative Commons Attribution-NonCommercial License (<https://creativecommons.org/licenses/by-nc/4.0/>), which permits non-commercial re-use, distribution, and reproduction in any medium, provided the original work is properly cited. For commercial re-use, please contact [journals.permissions@oup.com](mailto:journals.permissions@oup.com)

## Graphical Abstract



## Keywords

Watchman FLX • left atrial appendage • left atrial appendage closure • device-related thrombosis • cardiac computed tomography

## Introduction

Device-related thrombus (DRT) remains a significant complication following transcatheter left atrial appendage closure (LAAC) and appears on 1–5% of implanted devices, increasing the risk of thromboembolic complications.<sup>1–5</sup> DRT management involves an intensified course of anticoagulation and represents a clinical challenge due to the significant bleeding risk of LAAC patients.<sup>1</sup> An accurate diagnosis and treatment of DRT is critical to avoid thromboembolic complications, whereas overdiagnosis of DRT might lead to irrelevant intensified anticoagulation with an increased risk of bleeding.

Usually, DRT is detected during routine device surveillance, typically 6–12 weeks after LAAC.<sup>1</sup>

Although, transesophageal echocardiography (TEE) remains the most frequently used modality for follow-up imaging, cardiac computed tomography (CT) is increasingly utilized for both LAAC planning and follow-up.<sup>6,7</sup> An international expert consensus on the use of cardiac CT for preprocedural LAAC planning has been published.<sup>8</sup> However, a similar consensus regarding the evaluation and surveillance of DRT on postprocedural imaging does not exist.

We previously described a CT-based algorithm to discern hypoattenuated thickening (HAT) on the atrial device surface as part of device healing or DRT after LAAC with the Amplatzer Amulet device (Abbott, Lake Bluff, IL).<sup>9</sup>

In the present study, we sought to investigate and characterize HAT as seen by cardiac CT on the Watchman FLX device (Boston Scientific Inc., Marlborough, MA). Patient CT findings were correlated with imaging and histological data from experimental canine Watchman FLX implantations.

## Methods

## Study design

This retrospective single-centre analysis included all patients with successful Watchman FLX implantation and 8-week follow-up cardiac CT at Aarhus University Hospital, Denmark, between March 2019 and September 2021. As per institutional protocol, patients were discharged with either dual antiplatelet therapy (DAPT) or aspirin (ASA) monotherapy. Patients with a glomerular filtration rate >30 ml/min were scheduled for follow-up cardiac CT.

Baseline and procedure data were obtained from a local prospective registry of all consecutive LAAC procedures performed at Aarhus University Hospital, Denmark (n = 885). Patient files were reviewed in cases with high-grade HAT to confirm treatment and subsequent follow-up imaging. Clinical outcomes were defined according to the Munich consensus document and retrieved from individual patient files and through a search in the regional patient registry.<sup>10</sup> The study was conducted in accordance with the Declaration of Helsinki and approved by the Danish Data Protection Agency (1–16-02-419-16) and the Danish Patient Safety Authorities (3-3013-2736/1).

Pre-clinical animal data were provided by Boston Scientific, and examples of device healing and thrombosis were reviewed and compared to clinical findings. The preclinical protocol was approved by the Institutional Animal Care and Use Committee review board at American Preclinical Services (APS, Minneapolis, MN). The first, second, and last author had full access to all the included data and takes responsibility for its integrity and analysis.

## Cardiac CT protocol and analysis

The CT acquisition protocol has previously been described.<sup>8,9</sup> In brief, prospective electrocardiogram-gated CT acquisition was executed using a

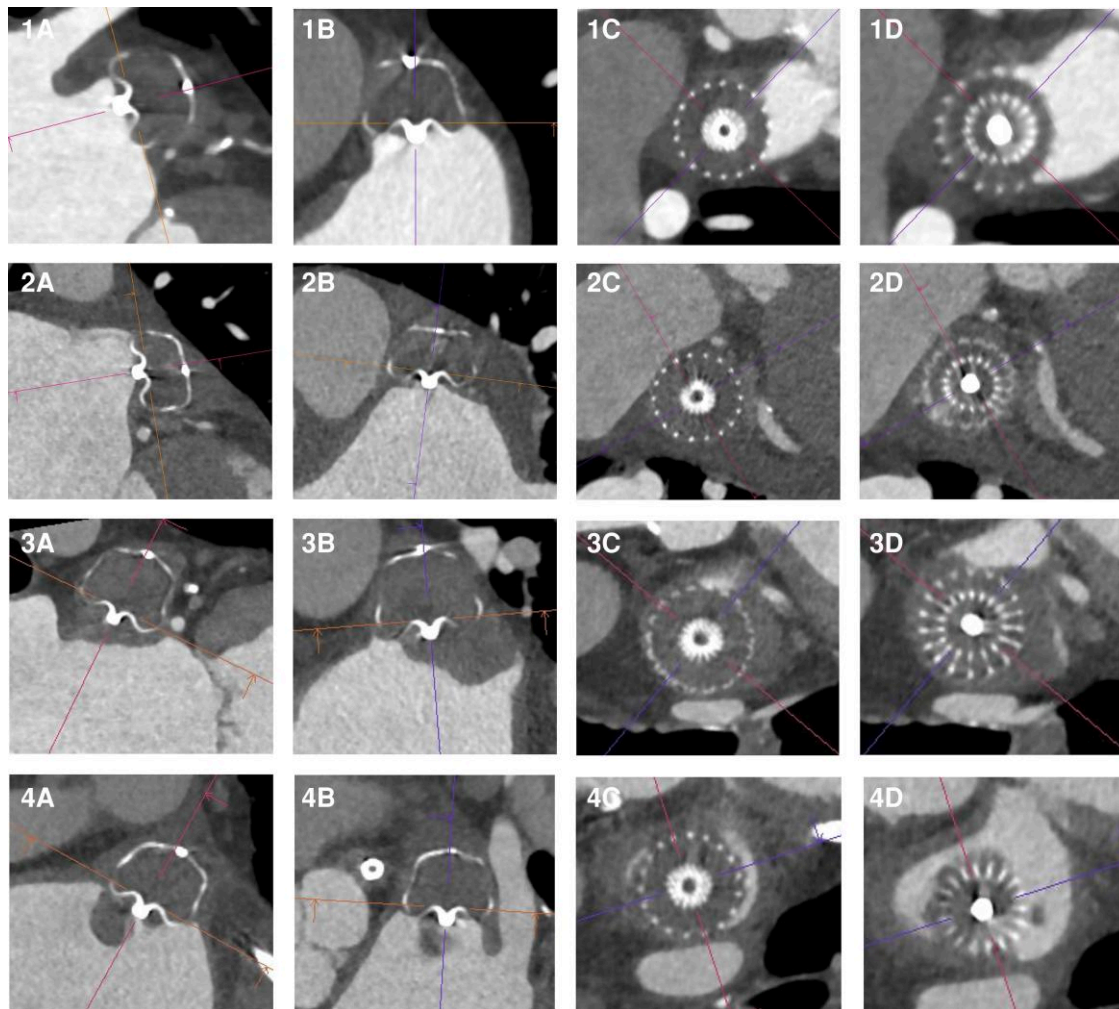


**Figure 1** Classification of HAT: classification of HAT based on cardiac CT performed 8 weeks after LAAC by the Watchman FLX device. The device was identified in a 30-degree right anterior oblique and 10-degree caudal view. The crosshair was then centred on the central device screw, and enface views were obtained by aligning the orthogonal planes with the central device screw hub and through the device shoulders at the level of the screw hub cove. (1A–D) Subfabric hypoattenuation; (2A–D) flat sessile HAT; (3A–D) protruding sessile HAT; (4A–D) pedunculated HAT.

high-pitch spiral protocol, iodine contrast, and a Siemens Somatom Definition Force scanner (Siemens Healthcare, Forchheim, Germany). A similar protocol was followed for preclinical scans. Additional details on CT acquisition can be found in the [Supplementary material](#).

Images were analyzed using the integrated imaging software syngo.via (Siemens Healthcare, Forchheim, Germany) by three investigators blinded to clinical outcomes. The implanted device was identified and analyzed through multiplanar views (*Figure 1*).

Cardiac CT was evaluated for the presence of device-related HAT, visual peridevice leak, and distal LAA contrast patency (see [Supplementary material](#)).

## HAT analysis

HAT was characterized based on localization, extent, and morphology. Localization was classified as either HAT on the device surface or isolated to the cove surrounding the screw hub. Extent was evaluated as any continuation onto the LA wall, the height of the HAT and of the screw hub cove. HAT height was measured from the atrial surface of the hypoattenuation to a line parallel to the bottom of the screw hub cove. The height of the

cove was defined as the distance from this line to the level of the most proximal frame (*Figures 1 and 2*).

Subsequently, based on a visual assessment of shape and homogeneity, HAT morphology was characterized as sessile or pedunculated. Sessile HAT was further subdivided into flat sessile ( $\leq 3$  mm) or protruding sessile ( $> 3$  mm) based on the height of the thickening (*Figure 1*). HAT in the screw hub cove was defined as isolated HAT with a height equal to or less than the height of the cove. Based on the design of the Watchman FLX device membrane, this was denominated as subfabric HAT (*Figure 2*).

The terminology and characterization of HAT is consistent with our previous study of HAT on the Amplatzer Amulet device but specifically modified according to the design differences between the Watchman FLX and Amulet.<sup>9</sup> Pedunculated HAT and protruding sessile HAT without continuity onto the LA wall and/or with an irregular surface was considered high-grade HAT.

## Preclinical data

The presented preclinical data ( $n=5$ ) is from a canine study (mongrel, 25–35 kg). Implantations were performed as per standard FLX protocol (See

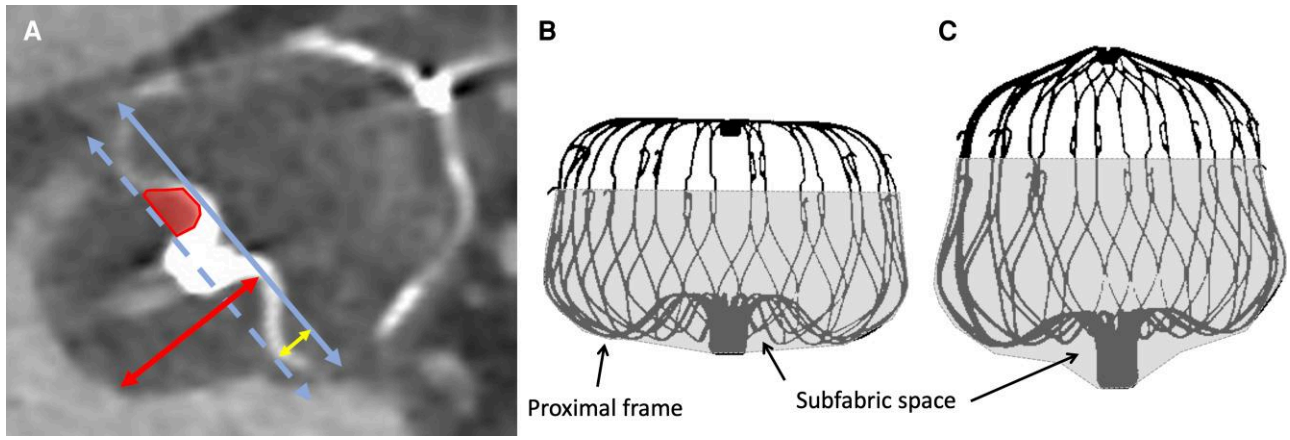


**Figure 2** Definitions and measures of hypoattenuation height: (A) measurements used in the classification and description of HAT on the atrial surface of the watchman FLX. In an approximated coronal cross section, a line (solid blue) is placed parallel to the bottom of the screw hub cover. Another line (dotted blue) is then placed at the level of the most proximal part of the frame. HAT present in the screw hub cover (red) between the blue lines is considered subfabric. The thickness of superficial HAT is then calculated by subtracting the height of the cove (small yellow arrow) from the total thickness of the HAT (large red arrow). (B) Uncompressed WATCHMAN with fabric (grey). (C) 11% compressed WATCHMAN resulting in an increased space between the frame and fabric (black arrow).

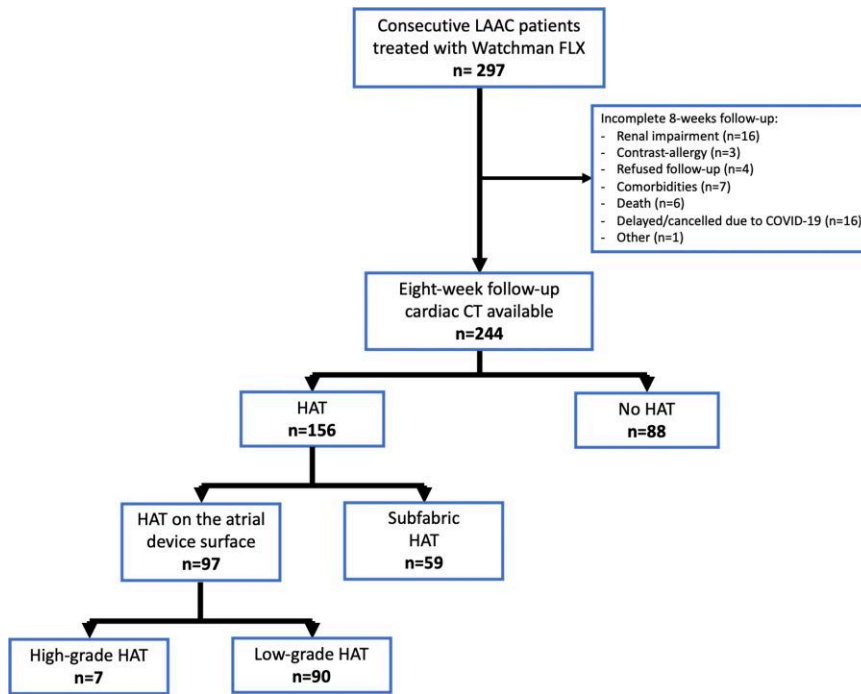


**Figure 3** Flow-chart of study patients and cases of HAT. COVID-19, coronavirus disease 2019.

Supplementary material). After 45 days, the heart was explanted, and a gross necropsy was performed. The left atrium was opened and enface pictures of the atrial device surface were obtained. Subsequently, the heart was fixed in formalin and prepared for histopathology. The device and LAA tissue were plastic embedded before medial, lateral, and central sections were cut. Standard haematoxylin/eosin and trichrome staining was performed on all sections.

**Statistical analysis**

Data distribution was evaluated using QQ-plots and histograms. Continuous variables are presented as mean with standard deviation (SD) or median with interquartile range (IQR) and compared using the two-sample t-test, Wilcoxon rank-sum, or analysis of variance as appropriate. Categorical variables are expressed as counts (percentages) and compared

**Table 1** Baseline characteristics of watchman FLX patients

	Incomplete CT follow-up n = 53	Study cohort n = 244	P-value
Age, years, mean (SD)	75.3 (8.1)	74.1 (8.8)	0.36
Sex, female	11 (20.8%)	72 (29.5%)	0.20
Body mass index, mean (SD)	25.7 (4.5)	27.6 (4.7)	0.008
Permanent atrial fibrillation	29 (54.7%)	109 (44.7%)	0.18
Renal insufficiency	34 (64.2%)	71 (29.1%)	<0.001
Stroke/TIA	16 (30.2%)	100 (41.0%)	0.14
Valvular heart disease	22 (41.5%)	74 (30.3%)	0.11
Diabetes mellitus	21 (39.6%)	48 (19.7%)	0.002
Ischaemic heart disease	24 (45.3%)	77 (31.7%)	0.059
Congestive heart failure	15 (28.3%)	42 (17.2%)	0.063
LVEF, median (IQR)	55.0 (45.0–60.0)	60.0 (50.0–60.0)	0.092
CHA <sub>2</sub> DS <sub>2</sub> -VASc, mean (SD)	4.3 (1.6)	4.0 (1.6)	0.16
HAS-BLED, mean (SD)	2.7 (1.0)	2.5 (1.1)	0.34
Indications for LAAC referral			
History of intracranial bleeding	6 (10.7%)	38 (15.8%)	0.34
History of GI bleeding	21 (37.5%)	66 (27.4%)	0.13
History of urinary tract bleeding	5 (8.9%)	19 (7.9%)	0.80
History of other spontaneous bleeding	8 (14.3%)	55 (22.8%)	0.16
Stroke despite OAC/NOAC	3 (5.4%)	22 (9.1%)	0.36
Cerebral Amyloid Angiopathy	0 (0.0%)	5 (2.1%)	0.28
Cognitive impairment	1 (1.8%)	2 (0.8%)	0.52
High Bleeding Risk	32 (57.1%)	130 (53.9%)	0.66
Preference/Compliance	3 (5.4%)	16 (6.6%)	0.72
Other	16 (28.6%)	56 (23.2%)	0.40
Discharge antithrombotic therapy			
Aspirin monotherapy	14 (26.4%)	80 (32.8%)	0.37
Clopidogrel monotherapy	1 (1.9%)	1 (0.4%)	0.23
Dual antiplatelet therapy	35 (66.0%)	159 (65.2%)	0.90
Other therapies	1 (1.9%)	1 (0.4%)	0.23
No antithrombotic therapy	2 (3.8%)	3 (1.2%)	0.19

Data are presented as mean ( $\pm$  SD), median (IQR) or numbers (%).

GI, gastrointestinal; LVEF, left ventricular ejection fraction; TIA, transient ischaemic attack.

using the Pearson's  $\chi^2$  or Fisher's exact test. Clinical follow-up data were analyzed using time-to-event analysis with Cox regression and presented as absolute events as well as incidence ratios. All statistical analyses were performed using STATA version 17 (StataCorp, College Station, TX).

## Results

During the study period, a total of 297 patients underwent LAAC with the Watchman FLX. Eight-week cardiac CT follow-up was available in 244 individuals (82.2%), constituting the study cohort (Figure 3).

Mean age was  $74.1 \pm 8.8$  years, 70.5% were males and the mean CHA<sub>2</sub>DS<sub>2</sub>-VASc and HAS-BLED scores were  $4.0 \pm 1.6$  and  $2.5 \pm 1.1$ , respectively.<sup>11,12</sup> Additional baseline characteristics are presented in Table 1. A total of 53 patients did not have CT follow-up. In 16 (30.2%), this was

due to renal failure, and in another 16 (30.2%), follow-up was not possible due to the COVID-19 pandemic (Figure 3). Median time from LAAC to follow-up CT was 55 days (IQR: 48–69), and the mean size of implanted devices was  $27.5 \pm 4.1$  mm (Table 2). The majority were discharged with either DAPT (65.2%) or ASA monotherapy (32.8%) (Table 1).

## HAT

HAT was seen in 156 (64%) of 8-week follow-up scans. In 59 (24.2%) of scanned patients, the HAT was classified as isolated subfabric hypoattenuation, constituting 38% of all HAT cases (Table 2). Among patients with HAT on the surface of the device ( $n = 97$ ), 78 (80.4%) were classified as flat sessile HAT, 17 (17.5%) as protruding sessile HAT, and 2 (2.1%) as pedunculated HAT. In total, seven patients were classified as having high-grade HAT features. We found no significant association between baseline patient characteristics, implantation details, or

**Table 2** Implantation characteristics of the study population

	Study cohort n = 244
Days since LAAC, median (IQR)	55.0 (48.0, 68.5)
Size of implanted device, mean (SD)	27.5 (4.1)
Device compression, mean (SD)	0.1 (0.1)
Peridevice leak	48 (19.7%)
LAA contrast patency	77 (31.7%)
LAA contrast patency without visible PDL	28 (11.5%)
Mid-device gap area, mm <sup>2</sup> , median (IQR)	42.5 (26.0–97.0)
HAT morphology	
No HAT	88 (36.1%)
Subfabric	59 (24.2%)
Flat sessile	78 (32.0%)
Protruding sessile	17 (7.0%)
Pedunculated	2 (0.8%)
Device lobe morphology	
Marshmallow	156 (63.9%)
Hot dog	20 (8.2%)
Bell	68 (27.9%)
Discharge antithrombotic therapy	
Aspirin monotherapy	80 (32.8%)
Clopidogrel monotherapy	1 (0.4%)
Dual antiplatelet therapy	159 (65.2%)
Other therapies	1 (0.4%)
No antithrombotic therapy	3 (1.2%)

Data are presented as mean ( $\pm$ SD), median (IQR) or numbers (%).

discharge antithrombotics with any type of HAT (see [Supplementary data online, Table S1](#)).

## Additional cardiac CT findings

In 19.7% of patients, a peridevice leak was identified on CT, displaying a median area at the mid-device level of 42.5 mm<sup>2</sup> (IQR: 26–97). Distal LAA contrast patency was present in 28 patients (11.5%) without any visible peridevice leak. Cardiac CT findings are summarized in [Table 2](#).

## Device-related thrombosis

Five patients with high-grade HAT (2 pedunculated, 3 protruding sessile) received intensified anticoagulation therapy for DRT based on their 8-week follow-up CT (see [Supplementary data online, Table S2](#)). The remaining two patients with high-grade HAT had protruding sessile HAT with either no LA wall continuity or an irregular surface ([Figure 3, Table 3](#)). Anticoagulation therapy was withheld in both due to multiple brain microbleeds and prior intracerebral haemorrhages.

Repeated follow-up imaging was scheduled by either cardiac CT ( $n = 4$ ) or TEE ( $n = 1$ ) in the patients treated with anticoagulation. Resolution was observed in three of five patients. One DRT patient died from pneumonia during extended follow-up, and another is awaiting further CT follow-up.

Of the 16 patients with protruding sessile HAT at 8-week follow-up, 10 patients (62.5%) were scheduled for additional follow-up imaging to monitor HAT development. No cases of flat sessile HAT were clinically considered as DRT ([Table 3](#)).

Mean follow-up time was  $1.4 \pm 0.8$  years. The overall number of events during follow-up was low, and no statistically significant differences in adverse event rates were found between HAT categories (see [Supplementary data online, Table S3](#)).

## Preclinical findings

Successful transcatheter Watchman FLX implantation was performed in all canines. On cardiac CT, a thin and smooth layer of HAT was observed across the surface of the device and in the screw hub cove, representing both subfabric and flat sessile HAT ([Figure 4](#)). One device ([Figure 4, Row 5](#)) presented with a contrast flow through the fabric.

Upon macroscopic evaluation, these findings correlated with a thin white pannus across the surface of the device, representing an ongoing healing process ([Figure 4](#)). Histology confirmed a thin layer of flattened cells with a typical endothelial morphology present across the device fabric for four of the five devices, while the remaining device ([Figure 4, row 5](#)) displayed only partial neoendothelization ([Figure 4](#) and see [Supplementary data online, Figures S1–S5](#)).

## Discussion

Cardiac CT has previously demonstrated increased sensitivity in detecting potential DRT when compared to TEE.<sup>9</sup> Additionally, the increased spatial resolution of cardiac CT enables detection and evaluation of subclinical findings such as low-grade HAT. An accurate diagnosis of DRT is essential in LAAC, but discrimination between potential DRT or benign device healing can be difficult.

In this retrospective, single-centre analysis we found HAT in any form to be present across a majority (64%) of Watchman FLX implants at 8-week follow-up CT scan. We further propose a classification and clinical algorithm for evaluation of HAT supported by histological findings in experimental animals.

## Subfabric hypoattenuation

In this study, subfabric HAT was observed in 24.2% of patients after Watchman FLX implantation. The Watchman FLX consists of a nitinol frame covered in part by a polyethylene terephthalate (PET) membrane. The individual nitinol struts are joined in a central screw hub, leaving a circular depression in the frame around the screw hub. Across the atrial device surface, the fabric is not tightly bound to each nitinol wire, resulting in a space underneath the fabric at the cove surrounding the screw hub. As the fabric is invisible on cardiac CT, contrast deficiencies in the screw hub cove can easily be mistaken for HAT across the atrial device surface. However, this cove is an intra-device space as clearly seen in our animal examples and subfabric hypoattenuation should not be mistaken for DRT ([Figure 4](#)). With increasing device compression, the fabric can even be lifted, further increasing the space between the fabric and the frame ([Figure 2](#)). Consequently, a straight line placed at the most proximal level of the device frame may underestimate the actual subfabric space. However, we propose this method as a conservative and reproducible approach.

## Suggested algorithm

For this study, we developed an algorithm for the analysis and interpretation of HAT ([Figure 5](#)). While the categories presented in this algorithm seem useful in identifying potential DRT, patient specific factors such as hypercoagulability, bleeding risk and comorbidities should be considered before intensifying anticoagulation in patients with protruding sessile or even pedunculated HAT.<sup>2</sup> Furthermore, additional factors

**Table 3** CT characteristics associated with low- and high-grade HAT

	Low-grade HAT n = 90	High-grade HAT n = 7	P-value
HAT morphology			<0.001
Flat sessile	78 (87%)	0 (0%)	
Protruding sessile	12 (13%)	5 (71%)	
Pedunculated	0 (0%)	2 (29%)	
HAT height above cove, mm, mean (SD)	2.1 (1.4)	7.9 (3.7)	<0.001
Smooth/uniform surface of HAT	86 (96%)	3 (43%)	<0.001
Continuation onto LA wall	75 (83%)	5 (71%)	0.42
Peridevice leak	12 (13%)	4 (57%)	0.003
LAA contrast patency	23 (26%)	4 (57%)	0.072
Mid-device gap area, mm <sup>2</sup> , median (IQR)	44.0 (33.0–102.0)	16.5 (14.0–57.5)	0.13
Distance from LUPV, mm, mean (SD)	12.1 (5.8)	23.8 (10.1)	<0.001
Size of implanted device, mean (SD)	27.4 (4.0)	28.3 (3.6)	0.59
Device area at screw hub, mean (SD)	505.2 (149.9)	513.0 (202.5)	0.90
Device compression, mean (SD)	10% (10%)	10% (10%)	0.42
Device lobe morphology			0.17
Marshmallow	67 (74%)	6 (86%)	
Hot dog	3 (3%)	1 (14%)	
Bell	20 (22%)	0 (0%)	
Discharge antithrombotic therapy			
Aspirin monotherapy	27 (30%)	2 (29%)	0.94
Dual antiplatelet therapy	60 (67%)	5 (71%)	0.80

Data are presented as mean ( $\pm$ SD), median (IQR) or numbers (%).  
LA, left atrial; LUPV, left upper pulmonary vein.

such as low-flow conditions, peridevice leak and implantation depth may be considered when deciding on increased anticoagulation or additional follow-up imaging.

Uneventful follow-up of patients with low-grade HAT on Amplatzer devices has previously been described, suggesting low-grade HAT to be a stage in the benign endothelialization of the atrial device surface.<sup>9</sup> While we lack paired human histology and imaging to confirm this, the canine data presented in this paper supports this interpretation.

## Device healing

In the setting of LAAC, the relationship between device healing, HAT and thrombosis remains incompletely understood. Limited evidence exists on explanted human devices.<sup>13,14</sup> However, a series of early animal studies have been performed using both disc- and plug-type devices.<sup>14–16</sup> As displayed in these studies, neoendothelialization is a time-dependent process, gradually progressing during the initial post-procedural months. While Bass<sup>15</sup> showed the surface of the disc-type Amplatzer Cardiac Plug (Abbott, Lake Bluff, IL) to be covered by stable neointima at 90 days, Kar et al.<sup>16</sup> showed incomplete endothelialization of the Amplatzer Cardiac Plug at 28 days post-procedure. In the latter study, the surfaces of all Watchman 2.5 devices were completely covered and incorporated at 28 days. Comparably, Schwartz et al. described complete coverage of the Watchman device at both 45 and 90 days.<sup>14</sup> Although the healing pattern was similar to that in canines, complete endothelialization was slower and less pronounced in humans.<sup>13,14</sup>

These differences relating to device design as well as varying degrees of endothelialization align with the pattern seen in the present analysis of HAT in a Watchman FLX population. At 8 weeks after LAAC, we found HAT on the surface of approximately 40% FLX implants, but only 6% HAT in a prior study of the Amulet device, suggesting that device healing might occur more rapidly for the FLX device.<sup>9</sup>

## Device-related thrombosis

Experienced clinicians found five of the included scans to represent DRT and initiated intensified anticoagulation therapy. Two additional patients showed high-grade HAT changes, but a clinical history with multiple intracerebral haemorrhages and microbleeds lead to a decision of observation without further anticoagulation therapy. The observed rate of DRT in this study (5/244; 2%) aligns our results with rates found in large registries and trials.<sup>1,3,4,17–19</sup>

Though this study was neither designed for nor powered to determine risk-factors for DRT, we found greater implant depths and peridevice leaks to be more common among patients with high-grade HAT (Table 3).

DRT remains a relatively rare complication and large registries are needed to substantiate these findings. However, the current evidence consistently underlines the continued importance of correct device positioning and thorough pre-procedural planning.<sup>1,2,20,21</sup>

Lastly, no association was found between discharge antithrombotic therapy and DRT. This was despite a large proportion of patients receiving only single antiplatelet therapy (33.2%), supporting previous observations of sufficient protection using this approach.<sup>18,22</sup>

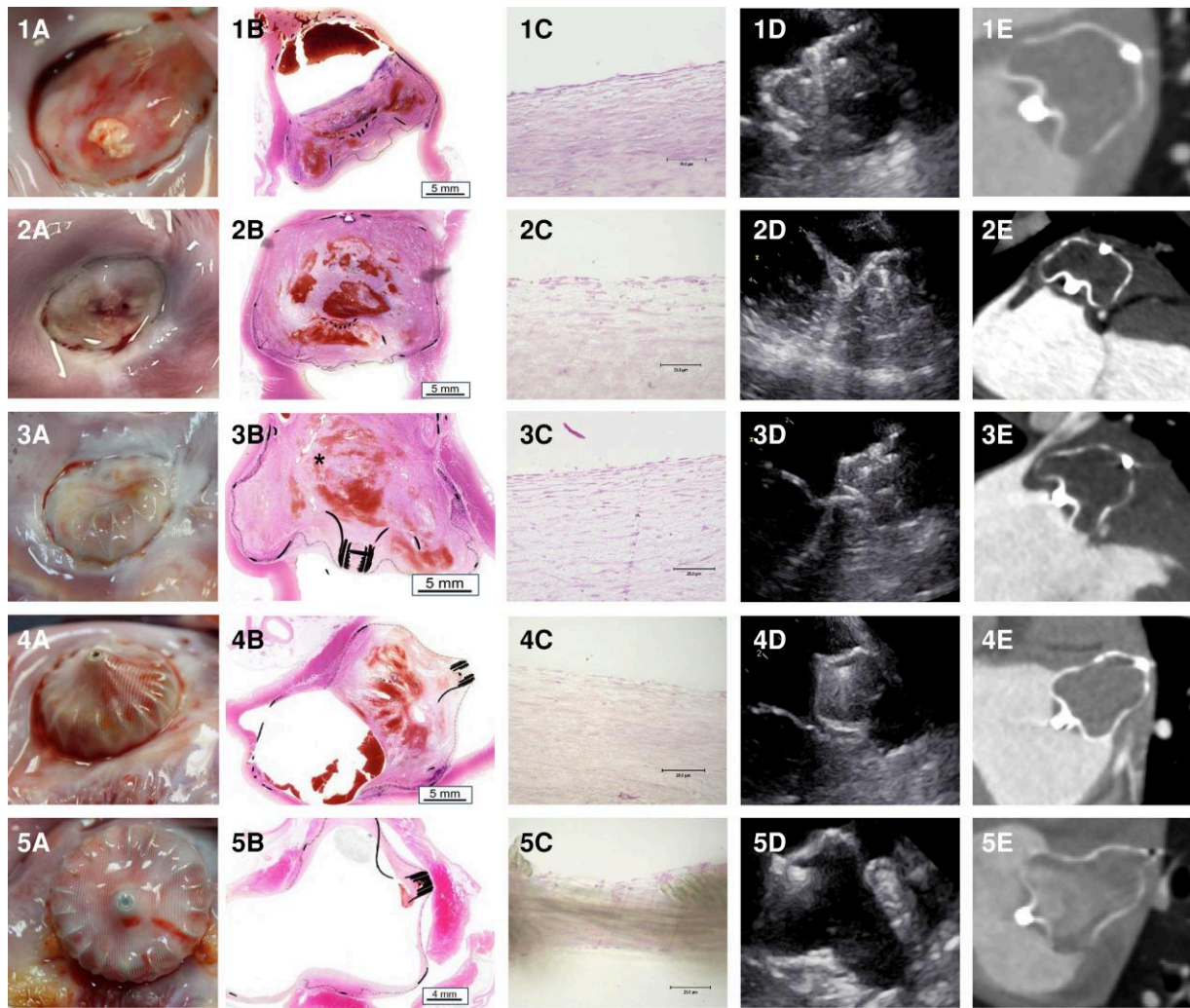


**Figure 4** Experimental animal data: explanted view (A), histology overview (B), high magnification image (400x) of neoendocardial surface (C) TEE (D) and cardiac computed tomography (E) from five separate canines (1–5) 45 days after device implantation. All TEEs shown are at 45-degree angles.

## Study limitations

Firstly, this is a single-centre study and thus represents the experiences within a high-volume LAAC setup at Aarhus University Hospital. Future studies will have to demonstrate the feasibility and translatability of the suggested algorithm.

As an observational study, elements of bias and confounding cannot be ruled out. However, analysis of all cardiac CT scans was performed blinded to the clinical interpretation and additional patient data to minimize this potential limitation. The low event rate during follow-up renders most statistical analyses of clinical outcomes underpowered. Also, most patients categorized as high-grade HAT were treated accordingly, potentially mitigating risk differences.

CT follow-up was only available for 82.2% of the study cohort, partially due to the reduced CT imaging capacity during the COVID-19 pandemic.

The study included only a limited number of canines with no representation of high-grade HAT.

Lastly, recent literature has shown a large proportion (~20%) of DRT-cases to present later than six months post-implantation.<sup>1</sup> This study included only data on short-term follow-up (median 55.0 days), as further imaging is not routinely performed at our institution.

## Conclusions

HAT is a frequent finding on CT imaging after LAAC with the Watchman FLX device. HAT can be classified into subfabric, flat sessile, protruding sessile, or pedunculated.

Subfabric hypoattenuation and flat sessile HAT are frequent findings for Watchman FLX, likely representing benign device healing. Pedunculated HAT and protruding HAT are infrequent CT findings that might represent DRT and should warrant additional therapeutic considerations.

Prospective evaluation of the proposed algorithm and of the clinical impact of HAT is warranted.

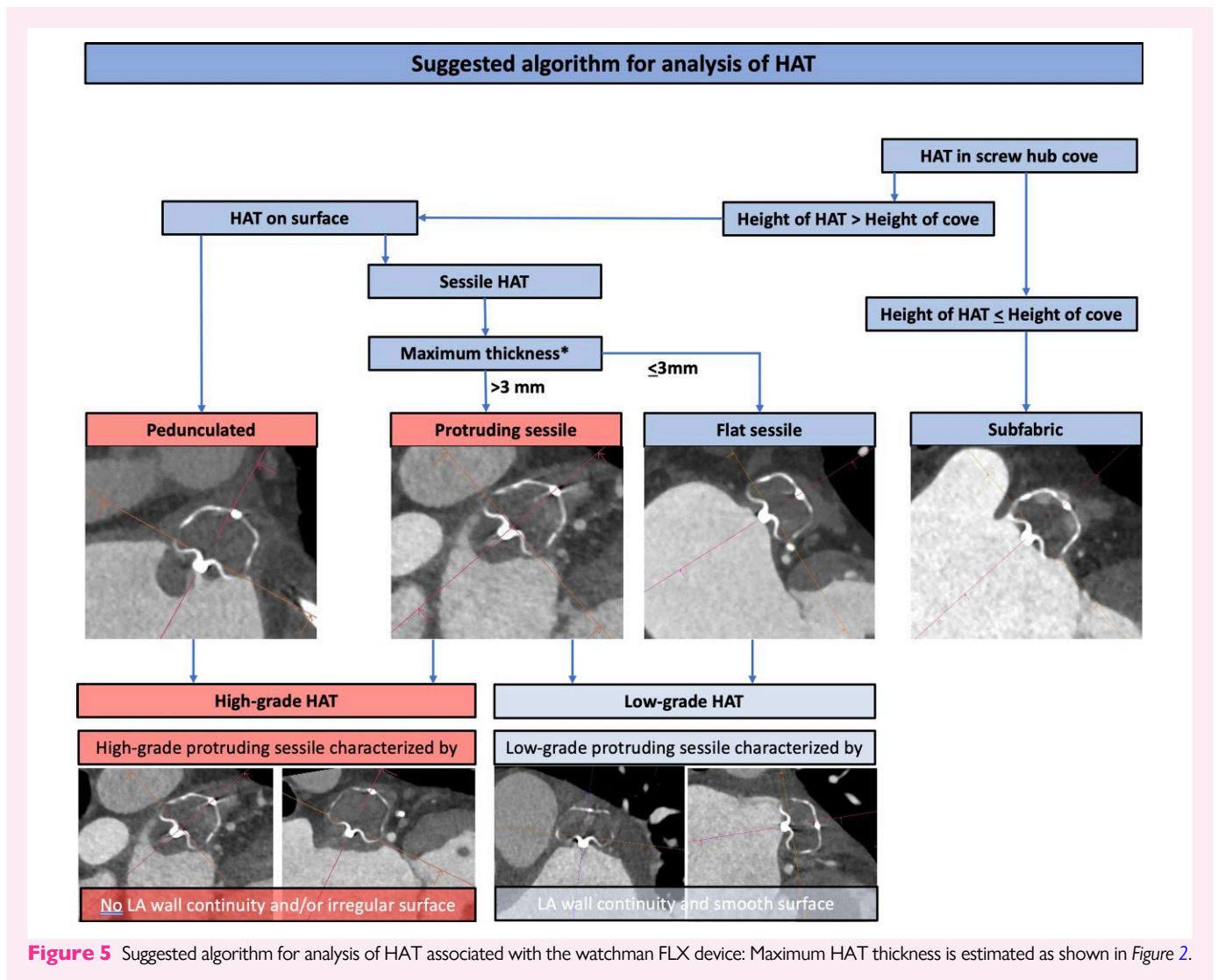
## Supplementary material

Supplementary materials are available at *European Heart Journal - Cardiovascular Imaging* online.

## Acknowledgements

The authors wish to acknowledge the contributions of Athanasios Samaras (AS) in the early phases of analysis and his inputs to the initial configurations of the REDCap database.





## Funding

Dr. Nielsen-Kudsk holds research grants from the Novo Nordisk Research Foundation (Hellerup, Denmark, NNF17OC0024868; NNF17OC0029510).

**Conflict of interest:** The preclinical experiments included in this study were supported by Boston Scientific. All analysis and interpretation of both clinical and preclinical data was carried out by the investigators. A.D.K. is currently enrolled as a PhD fellow at Aarhus University (Aarhus, Denmark) and has received a full scholarship from the institution. A.D.K. and J.M.J. have nothing to disclose. K.K. has received lecture fees from Abbott and Boston Scientific. B.L.N. has received institutional unrestricted research grants from HeartFlow. S.P. is an employee at Boston Scientific. R.H. is a consultant for Boston Scientific, Abbott and Biosense Webster and has received an educational grant from Baylis Medical. S.K. is a consultant for Boston Scientific, Abbott and WL Gore. J.S. is a proctor and consultant for and has received unrestricted research grants from Abbott and Boston Scientific. M.A. is on the advisory board of Boston Scientific and Abbott and has received research grants from Boston Scientific. J.E.N.-K. has received institutional research grants from Abbott and Boston Scientific.

## Data availability

The data underlying this article may be shared upon reasonable request to the corresponding author.

## References

- Sedaghat A, Vij V, Al-Kassou B, Gloekler S, Galea R, Fürholz M et al. Device-related thrombus after left atrial appendage closure: data on thrombus characteristics, treatment strategies, and clinical outcomes from the EURO-CARDIO-REGISTRY. *Circ Cardiovasc Interv* 2021;**14**:e010195.
- Simard T, Jung RG, Lehenbauer K, Pracon R, Jackson GG et al. Predictors of device-related thrombus following percutaneous left atrial appendage occlusion. *J Am Coll Cardiol* 2021;**78**:297–313.
- Aminian A, Schmidt B, Mazzone P, Berti S, Fischer S, Montorfano M et al. Incidence, characterization, and clinical impact of device-related thrombus following left atrial appendage occlusion in the prospective global AMPLATZER amulet observational study. *JACC Cardiovasc Interv* 2019;**12**:1003–14.
- Fauchier L, Cinaud A, Brigadeau F, Lepillier A, Pierre B, Abbey S et al. Device-related thrombosis after percutaneous left atrial appendage occlusion for atrial fibrillation. *J Am Coll Cardiol* 2018;**71**:1528–36.
- Dukkipati SR, Kar S, Holmes DR, Doshi SK, Swarup V, Gibson DN et al. Device-related thrombus after left atrial appendage closure. *Circulation* 2018;**138**:874–85.
- Korsholm K, Jensen JM, Nielsen-Kudsk JE. Cardiac computed tomography for left atrial appendage occlusion: acquisition, analysis, advantages, and limitations. *Interv Cardiol Clin* 2018;**7**:229–42.
- Saw J, Fahmy P, DeJong P, Lempereur M, Spencer R, Tsang M et al. Cardiac CT angiography for device surveillance after endovascular left atrial appendage closure. *Eur Heart J Cardiovasc Imaging* 2015;**16**:1198–206.
- Korsholm K, Berti S, Iriart X, Saw J, Wang DD, Cochet H et al. Expert recommendations on cardiac computed tomography for planning transcatheter left atrial appendage occlusion. *JACC Cardiovasc Interv* 2020;**13**:277–92.

9. Korsholm K, Jensen JM, Nørgaard BL, Nielsen-Kudsk JE. Detection of device-related thrombosis following left atrial appendage occlusion: a comparison between cardiac computed tomography and transesophageal echocardiography. *Circ Cardiovasc Interv* 2019;**12**:e008112.
10. Tzikas A, Holmes DR Jr, Gafoor S, Ruiz CE, Blomstrom-Lundqvist C, Diener HC et al. Percutaneous left atrial appendage occlusion: the Munich consensus document on definitions, endpoints, and data collection requirements for clinical studies. *Europace* 2017;**19**:4–15.
11. Lip Gregory YH, Robby N, Ron P, Lane Deirdre A, Crijns Harry JGM. Refining clinical risk stratification for predicting stroke and thromboembolism in atrial fibrillation using a novel risk factor-based approach. *Chest* 2010;**137**:263–72.
12. Ron P, Lane Deirdre A, Robby N, de Vos Cees B, Crijns Harry JGM, Lip Gregory YH. A novel user-friendly score (HAS-BLED) to assess 1-year risk of major bleeding in patients with atrial fibrillation. *Chest* 2010;**138**:1093–100.
13. Ellis CR, Alkhouli M, Anderson JA, Swarup V. Comparative endothelialization of amulet LAA occluder and watchman 2.5 LAA device. *J Am Coll Cardiol EP* 2022;**8**:828–9.
14. Schwartz RS, Holmes DR, Van Tassel RA, Hauser R, Henry TD, Mooney M et al. Left atrial appendage obliteration: mechanisms of healing and intracardiac integration. *JACC Cardiovasc Interv* 2010;**3**:870–7.
15. Bass JL. Transcatheter occlusion of the left atrial appendage—experimental testing of a new Amplatzer device. *Catheter Cardiovasc Interv* 2010;**76**:181–5.
16. Kar S, Hou D, Jones R, Werner D, Swanson L, Tischler B et al. Impact of watchman and Amplatzer devices on left atrial appendage adjacent structures and healing response in a canine model. *JACC Cardiovasc Interv* 2014;**7**:801–9.
17. Lempereur M, Aminian A, Freixa X, Gafoor S, Kefer J, Tzikas A et al. Device-associated thrombus formation after left atrial appendage occlusion: a systematic review of events reported with the watchman, the Amplatzer cardiac plug and the amulet. *Catheter Cardiovasc Interv* 2017;**90**:E111–e21.
18. Korsholm K, Nielsen KM, Jensen JM, Jensen HK, Andersen G, Nielsen-Kudsk JE. Transcatheter left atrial appendage occlusion in patients with atrial fibrillation and a high bleeding risk using aspirin alone for post-implant antithrombotic therapy. *EuroIntervention* 2017;**12**:2075–82.
19. Lakkireddy D, Thaler D, Ellis CR, Swarup V, Sondergaard L, Carroll J et al. Amplatzer amulet left atrial appendage occluder versus watchman device for stroke prophylaxis (amulet IDE): a randomized, controlled trial. *Circulation* 2021;**144**:1543–52.
20. Freixa X, Cepas-Guillen P, Flores-Umanzor E, Regueiro A, Sanchis L, Fernandez-Valledor A et al. Pulmonary ridge coverage and device-related thrombosis after left atrial appendage occlusion. *EuroIntervention* 2021;**16**:e1288–e94.
21. Sedaghat A, Schrickel JW, Andrie R, Schueler R, Nickenig G, Hammerstingl C. Thrombus formation after left atrial appendage occlusion with the Amplatzer amulet device. *JACC Clin Electrophysiol* 2017;**3**:71–5.
22. Rodriguez-Gabella T, Nombela-Franco L, Regueiro A, Jimenez-Quevedo P, Champagne J, O'Hara G et al. Single antiplatelet therapy following left atrial appendage closure in patients with contraindication to anticoagulation. *J Am Coll Cardiol* 2016;**68**:1920–1.